

Sintering Metal Nanoparticle Films

Howard Wang^{1*}, Liwei Huang¹, Zhiyong Xu¹, Congkang Xu¹, Russell J. Composto², Zhihao Yang³
¹Department of Mechanical Engineering, Center for Advanced Microelectronics Manufacturing, Binghamton University, SUNY, Binghamton, NY 13902

²Department of Materials Science and Engineering, University of Pennsylvania, Philadelphia, PA 19104

³NanoMas Technologies, Inc, Vestal, NY 13850

Email: wangh@binghamton.edu

Abstract

We have carried out several measurements in order to understand the process of metal nanoparticle (MNP) film sintering. Small angle neutron scattering has been used to reveal the average diameters of silver and gold nanoparticles (Ag-NPs and Au-NPs) used in this study to be 4.6 and 3.8 nm, respectively, with a size distribution of ca. 20%. Spin-cast Ag-NP and Au-NP films have been sintered at temperature ranges of 80 - 160 °C and 180 - 210 °C, respectively, for various times. The resulting film composition, morphology and electric resistance have been revealed. Upon sintering, the organic content in MNP films reduces to less than 10% while the overall film thickness reduces to about the half of the as-cast film thickness. The resistance of sintered Ag-NP films can vary over more than 7 decades depending on the sintering temperature. The conductivity of Ag-NP films sintered at 150°C is 2.4×10^{-8} Ωm. The transport properties are affected by both the composition and morphology of sintered films.

Keywords

Keywords, Metal nanoparticles, silver nanoparticles, sintering, printable electronics, ion beam analysis

1. Introduction

Printable electronics manufactured using roll-to-roll processes will offer the unique opportunities for mass production of large format and inexpensive flexible electronics [1]. A popular choice of the printable conductor precursor is metal nanoparticles (MNPs), which could be printed to substrates from solutions and sintered to conductive films at low temperatures because of the size effect [2]. Particularly, silver nanoparticles (Ag-NPs) are considered by many the most important precursor candidate for printed conductors for the good balance of cost and performance [3]. On the other hand, gold-nanoparticles (Au-NPs) are desirable because Au has better chemical stability and high work function. There have been extensive R&D efforts in developing methods for mass production of high quality Ag- and Au-NPs and exploring their applications in fabricating flexible devices [e.g., 3-6]. However, the understanding of the sintering process from precursor MNP to conductive metallic film is rather limited. In this paper, we report measurements in order to gain better understanding and better control of the MNP application to conductive film formation. This study is possible because high-quality and large quantities of uniform MNPs particles become available. By

applying a range of characterization methods including spectroscopic, thermal, microscopic and scattering techniques, we illustrate details of structures and behaviors of MNPs in both solution suspensions and deposited films. We try to gain fundamental understandings of nanomaterials processing in device applications. The insights in the sintering mechanism would offer guidance in materials design and processing

2. Materials

High-quality metal nanoparticles are obtained from NanoMas Technologies, Inc, who has developed synthesis routines for large scale production of silver and gold MNP with ultra-small particle size (2 to 10 nm) and narrow distribution. MNPs are stabilized with a thin layer of surfactant molecules, which also render MNPs soluble in non-polar organic solvents such as cyclohexane or toluene. UV-

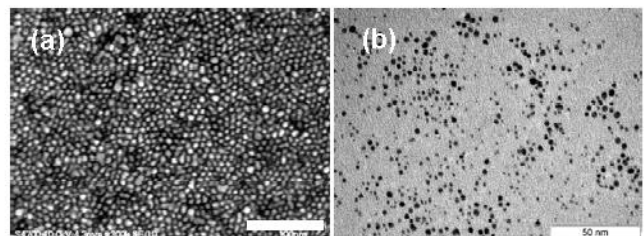


Fig. 1. (a) SEM micrograph of ca. 5 nm silver nanoparticles, and (b) TEM micrograph of ca. 4 nm gold nanoparticles.

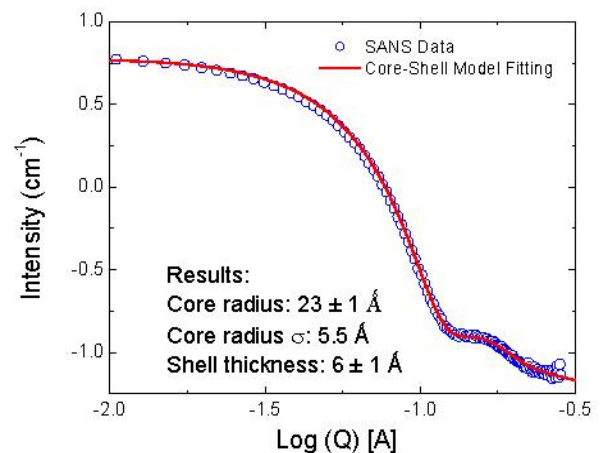


Fig. 2. Small angle neutron scattering of silver nanoparticles in deuterated toluene reveals an ensemble-averaged Ag core diameter of 4.6 nm with 20% dispersion, which is consistent with electron microscopy observation. The thickness of the organic shell is found to be ca. 0.6 nm in solutions.

visible absorption spectroscopy shows narrow absorption peaks centered at ca. 420 and 510 nm for Ag- and Au-NPs in dilute cyclohexane solutions, respectively. X-ray diffraction indicates that both MNPs have the same crystalline structures as the bulk metals. The size and uniformity of particles are examined using electron microscopy and small angle neutron scattering (SANS). Figure 1 shows a SEM micrograph of ca. 5 nm Ag-NPs (a), and a TEM micrograph of ca. 4 nm Au-NPs (b). SANS measurement of Ag-NP in toluene is shown in Fig. 2, in which the SANS data (open circles) are fitted with a core-shell model to give the average Ag-NP characteristics. The ensemble-averaged Ag-NP core diameter is found to be 4.6 ± 0.2 nm with a standard deviation dispersion of 1.1 nm, or $\pm 20\%$, which is consistent with electron microscopy observation. The thickness of the organic shell is found to be ca. 0.6 nm in solutions and 0.3 nm in the dried state. We emphasize the importance of characterizing bulk properties for achieving better performances in device applications.

3. Experiment

Films of Ag-NPs and Au-NPs were spun-cast from cyclohexane solutions with 10% and 5% MNP solid mass, respectively. MNP films were sintered in air at various temperatures for various times. As-cast and sintered films were characterized using ion beam analysis, electron microscopy, and direct-current I-V measurements. Two types of ion beam measurements were carried out using a collimated 2.0 MeV He^+ beam. The hydrogen content in the film was measured using forward recoil spectrometry (FRES), while the compositional profiles of heavier elements were measured using Rutherford backscattering spectrometry (RBS). In RBS, the incident beam was normal to the film, back scattered He ions were detected at 5° from the surface normal. In FRES, the incident beam was 75° from the surface normal, recoiled hydrogen atoms were detected at the specular reflection direction. Forward scattered He ions were stopped using an 8 μm thick Mylar foil.

3.1. RBS

Typical RBS spectra are shown in Fig. 3 for as-cast and annealed Au-NP films. The Au signals from the Au-NP films and Si signals from the substrates are clearly visible in Fig. 3a. Upon sintering, the width of Au peaks becomes narrower suggesting thinner Au-NP films (or more accurately smaller area atomic density) and the peak height increases indicating a higher Au density. The effect appears more prominent at the higher sintering temperature. Figure 3b is a blow-up view near the Si edges, where S signals are resolved. Since S is part of the thiol group binding the surfactant molecules to the Au-NP surfaces, the diminishing S signal upon sintering indicates that the hydrocarbon coating molecules have been driven away from the film. That causes the reduced area atomic density. Consequently, the Si front moves to the higher energies because of less energy loss for He^+ ions scattered off the Si at the substrate surface in annealed films.

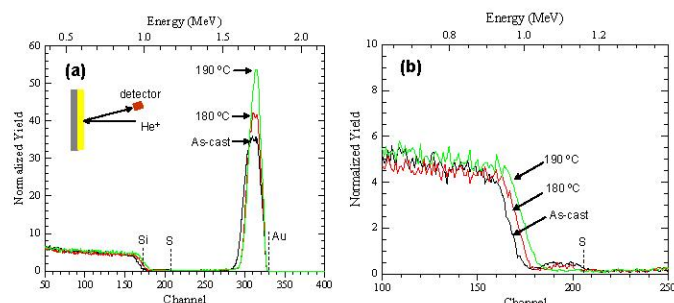


Fig. 3. (a) RBS spectra of Au-NP films showing increasing Au density upon sintering. (b) A blow-up view of the Si and S front showing diminishing S signals with sintering.

3.2. FRES

The loss of hydrocarbon coating molecules upon sintering is also evident from the FRES measurements. Figure 4a shows hydrogen peaks of FRES spectra of as-cast and sintered Ag- and Au-NP films. Figure 4a shows FRES spectra of Ag-NP films after various times at 80°C . The H-signal decreases with sintering time, indicating that sintering at a temperature as low as 80°C for a time as short as a few minutes is sufficient to drive majority of hydrocarbon away from the film. Figure 4b shows Au-NP films sintered at various temperatures for 3 min. Apparently, the variation of residual hydrocarbon content is sensitive only to a certain

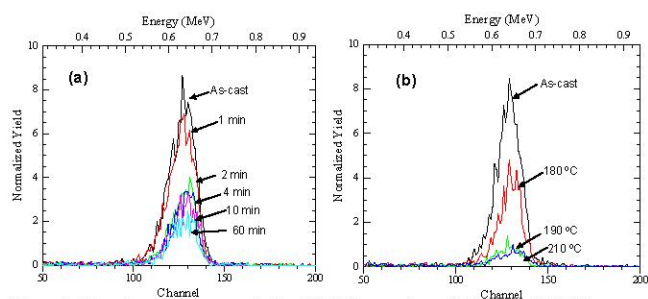


Fig. 4. The hydrogen peak in FRES spectra of (a) Ag-NP films sintered at 80°C for various times, and (b) Au-NP films sintered at various temperatures for 3 min. The H-content decreases with longer sintering time or higher sintering temperature.

range of sintering temperatures.

The fraction of residual hydrogen (equivalently the organic content) in sintered films is obtained from the integrated total H counts normalized by the as-cast ones. The time variations of residual H fraction in Ag-NP films sintered at 80°C and 100°C are shown in a semi-logarithm scale in Fig. 5a. The symbols are experimental data and the dashed lines are guide to the eye. The organic content decreases with the logarithmic sintering time, typically to below 10% after a few minutes at higher sintering temperatures. Figure 5b shows the residual H fraction in Au-NP films after sintered at various temperatures for 3 min. Apparently there is a transition regime between 170°C and 190°C . The organic content loss at 170°C is ca. 10%, while it becomes more than 90% at temperatures above 190°C . This behavior is due to a well-defined activation energy for the desorption of surfactant from Au-NP surfaces.

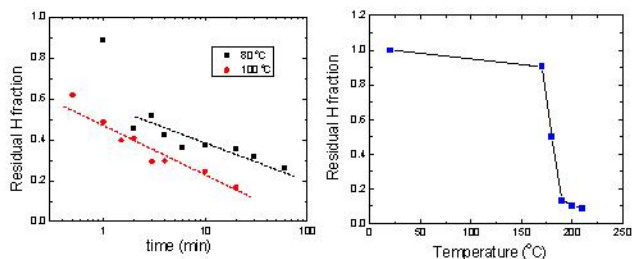


Fig. 5. The residual hydrogen analysis for (a) Ag-NP films sintered at 80 and 100 °C for various times, and (b) Au-NP films sintered at various temperatures for 3 min. The H-content decreases with longer sintering time or higher sintering temperature.

3.3. Morphology

Typical morphologies of sintered films are illustrated in Fig. 6. Sintered Ag-NP films usually are smooth with isolated holes, whereas sintered Au-NP films show long cracks. This could be understood since the volume reduction is larger in Au-NP films than in Ag-NP films. Thermal gravimetric analysis indicates that both Ag- and Au-NPs lose about 10% mass upon fully sintering. Since Au has higher density, the volume fraction of organics is higher in Au-NP films than in Ag-NP films. Upon sintering, larger volume shrinkage in Au-NP films causes higher tendency toward cracking than hole formation. For device application, crack morphology is not desirable since it would greatly deteriorate the electrical transport properties. A simple mending approach is printing multiple layers with sequential printing and sintering of each layer. Usually a second layer could improve the transport by 4 times to more than one order of magnitude. A challenging task is to control the volume shrinkage to occur normal to the film surface in stead of in lateral directions.

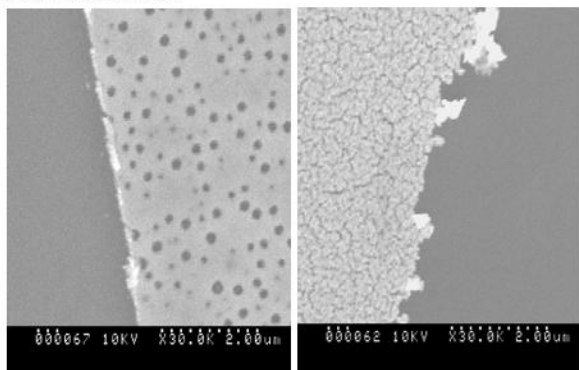


Fig. 6. SEM micrographs of (a) Ag-NP film after 5 min at 100 °C, and (b) Au-NP film after 6 min at 190 °C.

3.4. Resistance

Electric resistance measurements on sintered Ag-NP films are shown in Fig. 7. The time dependent resistance data as shown in Fig. 7a could be compared to the corresponding residual H content data in Fig. 5a. The comparison indicates that resistance of sintered film is sensitive to both the residual organic content and the sintering temperature. However, films with similar organic content at 80 °C and 100 °C can differ in electric resistance for several orders of magnitude. This observation suggests that morphology of sintered films

be critical in determining the transport properties. The morphology is in turn sensitive to particle characteristics and the thermal history.

The effect of sintering temperature is illustrated in Fig. 7b for Ag-NP films after 3 min sintering at various temperatures. The reduction of organic materials is of one decade at low and high temperatures, whereas the resistance varies over more than 7 decades. Furthermore, both residual H and resistance measurements indicate the somewhat optimal processing temperatures, ca. 200 °C for Au-NPs and ca. 130 °C for Ag-NPs, respectively.

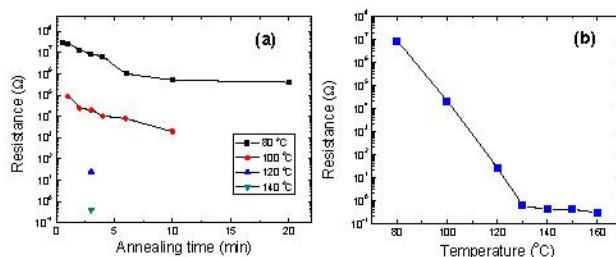


Fig. 7. The electrical resistance of Ag-NP films (a) sintered at various temperatures for various times, and (b) sintered at various temperatures for 3 min.

4. Conclusions

We have carried out a series of measurements in order to understand processes in sintering uniform metal nanoparticles. The composition, morphology and electric resistance of sintered Ag- and Au-NP films have been revealed. Upon sintering, the organic content in MNP films reduces to less than 10% while the overall film thickness reduces to half. The conductivity of Ag-NP films sintered at 150 °C was found to be $2.4 \times 10^{-3} \Omega\text{m}$. The transport properties are due mostly to the morphology of sintered films, which could vary due to particle characteristics and processing conditions.

Acknowledgments

This research was funded by the Center for Advanced Microelectronics Manufacturing at the State University of New York at Binghamton

References

1. Crawford, G. P. Ed. Flexible Flat Panel Display, Wiley (2005)
2. Buffat, Ph., Borel, J-P., "Size Effect on the Melting Temperature of Gold Particles", Phys. Rev. A, 13, pp 2287-2298, 1976.
3. Gasman, L., "Silver Powders and Inks for Printable Electronics 2007-1014", NanoMarkets report NA-3022, 2007.
4. Park JW, Baek SG., "Thermal Behavior of Direct-Printed Lines of Silver Nanoparticles", Scripta Materialia, 55, pp 1139-1142, 2006.
5. Wakuda D, et. al. "Novel Method for Room Temperature Sintering of Ag Nanoparticle Paste in Air", Chem Phys. Lett, 441, pp 305-308, 2007.
6. Kim, D. et. al. "Ink-Jet Printing of Silver Conductive Tracks on Flexible Substrates", Mol. Cryst. Liq. Cryst., Vol. 459, pp. 45-55, 2006